Molecular BioSystems

Accepted Manuscript

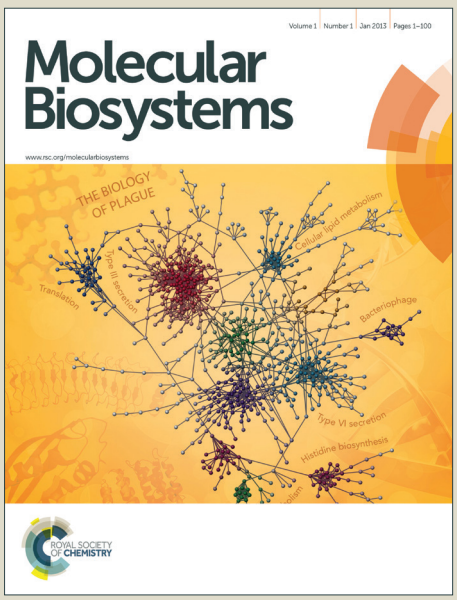

ROYAL SOCIETY OF CHEMISTRY

www.rsc.org/molecularbiosystems

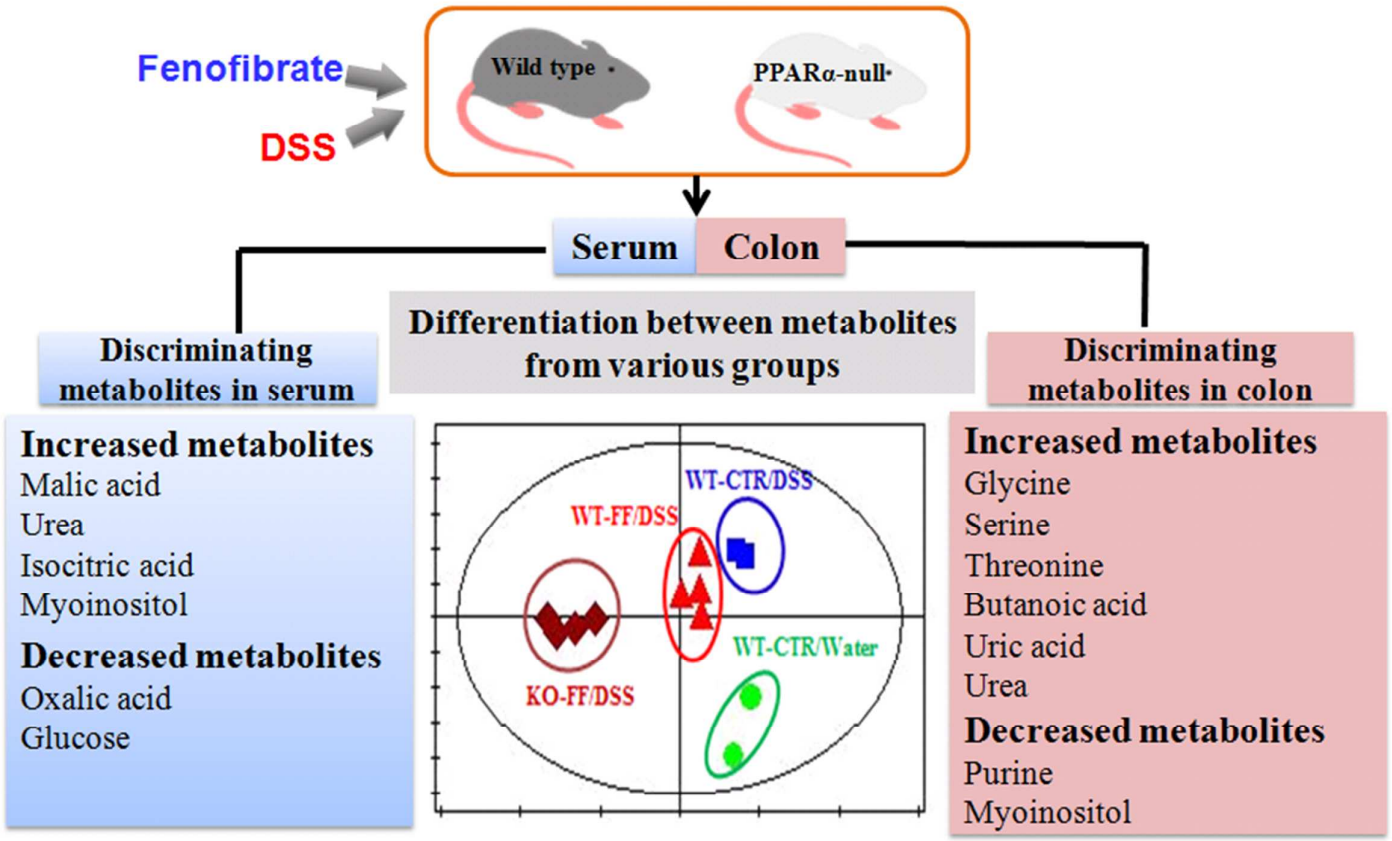

GC-MS metabolomics revealed discriminating metabolites in serum and colon of colitis mice to decipher the PPARα-dependent exacerbation of colitis.

GC-MS metabolomics on PPARα-dependent exacerbation of colitis

Xueqin Gu[1,2], Yunlong Song[1], Yifeng Chai[1], Feng Lu[1], Frank J. Gonzalez[3], Guorong Fan[1,*], Yunpeng Qi[1,2,*]

[1]School of Pharmacy, Second Military Medical University, Shanghai 200433, China
[2] Fujian University of Chinese Traditional Medicine, Fuzhou, Fujian 350122, China
[3]Laboratory of Metabolism, Center for Cancer Research, National Cancer Institute, National Institutes of Health, Bethesda, Maryland 20892, USA

Corresponding author:
Yunpeng Qi, Department of Pharmaceutical Analysis, School of Pharmacy, Second Military Medical University, Shanghai 200433, China.
E-mail: qiyunpeng@smmu.edu.cn; Fax: 86-21-81871265; Tel: 86-21-81871265.
Guorong Fan, Department of Pharmaceutical Analysis, School of Pharmacy, Second Military Medical University, Shanghai 200433, China.
E-mail: guorfan@outlook.com; Fax: 86-21-81871260; Tel: 86-21-81871260.

Running title:
GC-MS metabolomics on PPARα-dependent exacerbation of colitis.

Abbreviations:

DSS, dextran sulfate sodium; IBD, inflammatory bowel disease; PLS-DA, partial least squares-discriminant analysis; VIP, variable influence on projection; PCA, principal components analysis; PPARα, peroxisome proliferator-activated receptor α; SM, sphingomyelin; TNBS, trinitrobenzene sulfonic acid; MSTFA, N-methyl-(trimethylsilyl)trifluoracetamide; TMCS, chlorotrimethylsilane; GC/MS, gas chromatography coupled to mass spectrometry; THA, threonine aldolase; PSAT1, phosphoserine aminotransferase 1.

Abstract

Fenofibrate, a peroxisome proliferator-activated receptor α (PPARα) agonist, was found to exacerbate inflammation and tissue injury in experimental acute colitis mice. Through lipidomics analysis, bioactive sphingolipids were significantly up-regulated in the colitis group. In this study, to provide further insight into the PPARα-dependent exacerbation of colitis, gas chromatography-mass spectrometry (GC/MS) based metabolomics was employed to investigate the serum and colon of dextran sulfate sodium (DSS)-induced colitis mice treated with fenofibrate, with particular emphasis on changes in low-molecular-weight metabolites. With the aid of multivariate analysis and metabolic pathway analysis, potential metabolite markers in amino acid metabolism, urea cycle, purine metabolism, and citrate cycle were highlighted, such as glycine, serine, threonine, malic acid, isocitric acid, uric acid, and urea. The level changes of these metabolites in either serum or colons of colitis mice were further potentiated following fenofibrate treatment. Accordingly, expression of threonine aldolase and phosphoserine aminotransferase 1 was significantly up-regulated in colitis mice and further potentiated in fenofibrate/DSS-treated mice. It was revealed that beyond control of lipid metabolism, PPARα also shows effects on the above pathways, resulting in enhanced protein catabolism and energy expenditure, increased bioactive sphingolipid metabolism and proinflammatory state, which were possibly related to the exacerbated colitis.

Keywords: peroxisome proliferator-activated receptor α; GC/MS; metabolomics; fenofibrate; colitis

INTRODUCTION

Inflammatory bowel disease (IBD), including ulcerative colitis (UC) and Crohn's disease (CD), is a group of chronic inflammatory conditions affecting the gastrointestinal tract[1]. Epidemiological studies revealed that the incidence rate of IBD has markedly increased worldwide, with the highest reported incidence in North America and Europe[2, 3]. Previous studies suggested that IBD is associated with immunological disorders caused by genetic, environmental, and microbiological factors[4, 5]. However, the accurate etiology of IBD still remains to be understood.

Peroxisome proliferator-activated receptor α (PPARα) is a nuclear hormone receptor that transcriptionally regulates lipid metabolism, atherosclerosis, and inflammation[6-8]. In a previous study using PPARα-null mice, fenofibrate, the clinically used hyperlipidemic drug (a PPARα agonist), was found to exacerbate inflammation and tissue injury in experimental acute colitis mice under three distinct protocols, dextran sulfate sodium (DSS), trinitrobenzenesulfonic acid (TNBS), and Salmonella Typhi[9]. Lipidomic analysis revealed that bioactive sphingolipids, including sphingomyelins (SM) and ceramides, were significantly increased in the colitis group compared to the control group, which was further potentiated following fenofibrate treatment. This study indicated that decreased hydrolysis and increased synthesis of SM, upregulated RIPK3-dependent necrosis, and elevated mitochondrial fatty acid β-oxidation, were possibly related to the exacerbated colitis[9].

In the above lipidomics study, lipids such as sphingolipids were expectedly highlighted since they have emerged as important signaling molecules regulating inflammatory responses; also, a primary action of PPARα activation is the transcriptional regulation of genes involved in lipid metabolism[10]. Besides lipids, other low-molecular-weight metabolites, such as amino acids, bile acids, and fatty acids, were also closely correlated with IBD[11-13]. For example, both UC and CD were found to have an impact on amino acid metabolism, and levels of certain amino acids and citrate acid (TCA) cycle-related molecules were changed in colitis mice or UC patients[14-16]; malabsorbed bile acids in the colon cause diarrhea in pediatric IBD patients[17]; and alterations in the expression of genes involved in intestinal fatty acid

metabolism in IBD patients were identified[18]. Beyond lipids, PPARα was also revealed to regulate amino acid metabolism by influencing the expression of several genes involved in trans- and deamination of amino acids and urea synthesis[19]. However, little was reported concerning the comprehensive perturbation and interaction of PPARα activation and colitis on the low-molecular-weight metabolites such as amino acids. Hence, the aim of the present study was to provide further insight into effects of the PPARα agonist (fenofibrate) in colits mice, with particular emphasis on changes in low-molecular-weight metabolites, to further decipher the PPARα-dependent exacerbation of colitis.

Metabolomics aims to identify and quantify the metabolites that serve as substrates and products in metabolic pathways in response to physiologic perturbations[20, 21]. Mass spectrometry (MS) and nuclear magnetic resonance (NMR) are commonly applied in metabolomics study[22]. Among them, gas chromatography coupled to mass spectrometry (GC/MS) is widely used for profiling low-molecular-weight metabolites such as amino acids and fatty acids in various biofluids, outperforming other technical platforms due to its high sensitivity and reproducibility, as well as the availability of electron impact (EI) spectral libraries for structural identification[23-26]. In this study, GC-MS was used to characterize the metabolic profiles of the experimental colitis mice subjected to DSS and treated with fenofibrate. With the aid of multivariate analysis methods and metabolic pathway analysis, new hints on the roles of fenofibrate on colitis were explored and revealed.

MATERIALS AND METHODS

Chemicals and reagents. Methoxylamine hydrochloride, *N*-methyl-(trimethylsilyl) trifluoracetamide (MSTFA), chlorotrimethylsilane (TMCS), pyridine and ribitol (used as internal standard), and all the authentic standards were purchased from Sigma-Aldrich (St. Louis, MO, US). Methanol and acetonitrile were purchased from TEDIA (Fairfield, OH, USA). Dextran sulfate sodium (DSS) was purchased from MP Biomedicals (Solon, OH, USA) (MW=36000-50000).

Mice and treatments. All animal treatments in this study were approved by the

National Cancer Institute of National Institute of Health, USA. Wild-type and PPARα-null, 6-to-8-week-old male C57BL/6J mice were fed either standard diet or modified diet containing 0.1% fenofibrate *ad libitum* (Bioserv, Frenchtown, NJ) three days before the experiment and through the end of the study. Colitis was induced by the addition of drinking water containing 3.0% (wt/vol) DSS for 7 days. The presence of fenofibrate in the diet did not affect food or water intake as compared to the control groups not administered the drug. The mice were killed 7 days after DSS administration and after 8 h of overnight fasting. Serum samples were collected by retro-orbital bleeding, and tissue samples were harvested and stored at -80 ℃ before analysis.

Colitis evaluation. Body weights of the mice were recorded daily. Assessment of diarrhea, rectal bleeding, and bloody stool daily were reported as a score from 0 to 4. The histological examination of the colon tissue was performed by blinded analysis and the severity of colon damage was determined by a routine hematoxylin and eosin (H&E)-stained section according to the morphological criteria described previously[27, 28].

Metabolomics. For serum metabolomics analysis 30 μl serum were mixed with 4-fold acetonitrile solution containing 10 μl ribitol (0.04 mg/mL) as internal standard. The solution was vortexed for 30 s and sonicated for 10 min, and the resultant supernatant collected after being centrifuged at 10000 rpm for 10 min at 4 ℃. The supernatant was dried using a vacuum concentrator (ThermoFisher, USA). For oximation, 30 μl methoxyamine hydrochloride (15 mg/mL) dissolved in pyridine were mixed with the dried sample before being heated for 1 h at 60 ℃. Next, 90 μl MSTFA (containing 1% TMCS) were added for derivatization and the mixture was also heated for 1 h at 60 ℃. The mixture was then centrifuged at 10000 rpm for 10 min after being cooled and the resultant supernatant was subjected to GC/MS analysis. For colon tissue metabolomics analysis, about 20 mg accurately weighted tissues were homogenized with 50-fold methanol solution containing ribitol (0.04 mg/mL) as internal standard. The mixture was then centrifuged at 10000 rpm for 10 min after 10 min of ultrasound. 800 μl of the supernatant was collected and then was dried. Oximation and the

subsequent derivatization were performed using 30 μl methoxyamine hydrochloride (15 mg/mL) and 90 μl MSTFA (containing 1% TMCS) as described above and the resultant supernatant was subjected to GC/MS analysis.

For metabolomics discovery, the derivatized samples were analyzed on a Thermo Scientific ITQ 1100^{TM} GC/MS^{n} (ThermoFisher Electron Corporation, USA) with a GL-5MS column (30 m × 0.25 mm i.d.; film thickness 0.25 μm) (GL Sciences, Inc. Japan) under the following conditions: the initial oven temperature was set at 70 ℃, ramped to 150 ℃ by 5 ℃/min, then risen from 150 ℃ to 200 ℃ by 3 ℃/min and held for 2 min, finally, ramped to 280 ℃ by 10 ℃/min and held for 2 min. 1.0 μl of sample solution was injected with split mode (the split ratio 30:1), with helium as the carrier gas at a flow of 1.0 mL/min. The temperature of injector, ion source and transfer line were 250 ℃, 220 ℃, 250 ℃, respectively. The electron energy was 70 eV. The mass spectrometer was operated in full scan mode from 50 to 1000 m/z and the solvent delay was set at 5 min.

For metabolite identification, the GC-MS spectra was subjected to searching using the NIST (National Institute of Standards and Technology) database installed in an ITQ 1100^{TM} GC/MS^{n} system. To confirm the identities of the putative markers, mass spectra of the metabolites were compared with those of the available authentic standards. To ensure the stability of the GC/MS system, an equal volume of each sample was pooled together to generate a pooled quality control (QC) sample. This QC sample was processed in the same way as the real samples and then run randomly through the analytical batch. Concentrations of the metabolites in the samples were determined based on standard curves using authentic standards.

Multivariate data analysis and metabolic pathway analysis. The acquired GC-MS data was first converted into CDF format. XCMS (https://xcmsonline.scripps.edu/) was used for nonlinear alignment of the data in the time domain and automatic integration and extraction of the peak intensities, using default GC/Single Quad parameters. The XCMS output data was first normalized by dividing by the internal standard peak using the Microsoft Excel software, and then loaded to SIMCA-P software (Umetrics, Kinnelon, NJ) and transformed by mean-centering and pareto

scaling, the technique that increases the importance of low abundance ions without significant amplification of noise. Statistical models including principal components analysis (PCA) and partial least squares-discriminant analysis (PLS-DA) were established to represent the major latent variables in the data matrix. The discriminating metabolites were obtained using a statistically significant threshold of variable influence on projection (VIP) values obtained from the PLS-DA model where the metabolites with VIP values higher than 1 were selected.

Metabolic pathway analysis was performed by MBRole[29] based on the database sources including KEGG (http://www.genome.jp/kegg/), Human Metabolome Database (http://www.hmdb.ca/), and PubChem (http://www.ncbi.nlm.nih.gov /pccompound/) to identify the affected metabolic pathways and facilitate further biological interpretation.

RNA analysis. RNA was extracted using TRIzol reagent (Invitrogen). Quantitative real-time PCR (qPCR) was performed using cDNA generated from 1 μg total RNA with the SuperScript II Reverse Transcriptase kit (Invitrogen). Primers were designed for qPCR using Primer Express software (Applied Biosystems, Foster City, CA) and sequences are available upon request. qPCRs were carried out using SYBR green PCR master mix (Applied Biosystems) in an ABI Prism 7900HT Sequence Detection System (Applied Biosystems). Values were quantified using the comparative threshold cycle method, and samples were normalized to GAPDH.

Data analysis. Experimental values were expressed as mean±S.D. Statistical analysis was performed using Prism 6.0 (GraphPad Software, Inc., San Diego, CA). Repeated measures analysis of variance (ANOVA) with posthoc test, two-way ANOVA, and Mann-Whitney test were used to evaluate the significance of differences between the groups where necessary. A *p*-value below 0.05 was considered statistically significant.

RESULTS

GC-MS metabolomics analysis of experimental colitis induced by DSS. DSS treated mice had significantly decreased body weights and other signs of intestinal injury including rectal bleeding, diarrhea, shorter colon length and inflammation and

epithelial degeneration. Upon treatment with a fenofibrate-supplemented diet, wild-type (WT) mice treated with DSS displayed a more severe colitis, whereas fenofibrate-treated PPARα-null mice were less susceptible to colitis[9] (Body weight data of the mice were shown in Table.S1. Body weight figures, colon lengths, rectal bleeding and diarrhea scores, and images of hematoxylin and eosin-stained colon tissues of the mice can be found in our recent publication at: *Am J Physiol Gastrointest Liver Physiol 307: G564–G573, 2014*). These results indicated that fenofibrate treatment exacerbates tissue injury and inflammation in colitis mice, possibly dependent on PPARα activation.

In this study, GC-MS based metabolomics was performed to discover other metabolite markers than lipids to gain mechanistic insight into the exacerbation of colitis by fenofibrate treatment. In serum, PCA scores plot showed distinct clustering for the four groups, *i.e.*, control-treated WT mice, DSS-treated WT mice, fenofibrate/DSS-treated WT and PPARα-null mice, with the cumulative R^2X 0.659 and Q^2 0.543 for this model (Figure 1A). Similarly, the PLS-DA scores plot exhibited clear separation among the four groups with the cumulative R^2X 0.771, R^2Y 0.841, and Q^2 0.442 (Figure 1B). In colon, both PCA (R^2X 0.602 and Q^2 0.196) (Figure 1C) and PLS-DA scores plot (R^2X 0.818, R^2Y 0.99, and Q^2 0.763) (Figure 1D) showed distinct clustering and clear separation for the four groups, too. These results indicated that from the view of metabolomics, the phenotypes of the four groups could be clearly distinguished, in accordance with the previous pathological findings[9].

Identification and quantitation of the potential metabolite markers. The common way to screen the potential markers related to diseases is to compare the control and disease groups and then screen the differentiating metabolites. Based on the PLS-DA models (for serum and colon, respectively) discriminating the control and colitis groups, a bunch of significantly altered ions were revealed (Figure S1), and were later identified as metabolites listed in Table 1. It could be observed that the altered metabolites in serum and colon were quite different.

In the QC samples, for all the metabolites listed in Table.1, the relative standard deviation (RSD) ranged from 0.06% to 0.42% for the retention times and ranged from

2.39 % to 5.21% for the peak areas, which demonstrated the robustness of the method. Relative levels of the potential metabolite markers in serum and colon of the four groups were shown in Figure 2 (fold changes compared to the control group). In serum of DSS-treated WT mice, malic acid and urea levels were significantly increased but oxalic acid and glucose levels were decreased compared to the control mice. In colon, compared to the control mice, amino acids including glycine, serine, and threonine, as well as butanoic acid, uric acid, and urea were increased while purine and myoinositol were decreased in colitis mice. All the above trends of the metabolites in serum or colon were further potentiated in fenofibrate/DSS-treated WT mice other than in PPARα-null mice. The level fluctuations of these potential metabolite markers, especially those apparently correlated with fenofibrate treatment, may provide clues for investigating the exacerbation of fenofibrate on experimental colitis.

Metabolic Pathway Analysis. A functional enrichment analysis facilitating further biological interpretation was subsequently performed using MBRole to reveal the most relevant pathways. It was shown in Table S2 that the revealed metabolite markers were mainly involved in the following pathways: purine metabolism (uric acid, glycine, and urea), glyoxylate and dicarboxylate metabolism (malic acid, isocitric acid, and oxalic acid), aminoacyl-tRNA biosynthesis (threonine, serine, and glycine), glycine, serine and threonine metabolism (glycine, threonine, and serine), galactose metabolism (glucose, myoinositol), and citrate cycle (isocitric acid, malic acid).

***Analysis of gene expression in the serine, glycine and threonine pathway*.** According to Table 1 and Table S2, some metabolites together with the involved pathways were revealed to be probably associated with colitis and the PPARα-dependent exacerbation. Afterwards, expression of some key genes in these pathways were evaluated in colon samples of various groups using qPCR, among which threonine aldolase (THA) and phosphoserine aminotransferase 1 (PSAT1) were significantly up-regulated in colitis mice compared to control mice, and further potentiated in fenofibrate/DSS-treated WT mice (Figure 3). These observations

supported our metabolomics findings as will be discussed below[30, 31].

DISCUSSION

In this study, a GC/MS-based metabolomics approach was performed on serum and colon tissues of DSS-induced colitis mice treated with fenofibrate. Levels of several metabolite markers were altered in control, colitis, and fenofibrate/DSS-treated WT or PPARα-null mice. Among them, malic acid, glycine, serine, threonine, uric acid, and urea were increased in either serum or colons of colitis mice, whereas oxalic acid, glucose, purine, and myoinositol were decreased. Upon treatment with a fenofibrate-supplemented diet, these trends were potentiated in WT mice other than PPARα-null mice. These metabolites with further potentiated levels after fenofibrate treatment (but not in KO-FF/DSS group) may possibly be related to PPARα activation, and hence could provide clues for investigating the exacerbation of fenofibrate on experimental colitis. Though some metabolites, such as serum urea, had similar levels in WT-CTR/DSS and KO-FF/DSS groups, these two groups could not be directly compared since their biological backgrounds were totally different. WT-CTR/DSS mice were in the basal physiological status whereas the KO-FF/DSS group were knockout mice. The similar levels of some metabolites in these two groups may partly due to both groups had colitis. Through metabolic pathway analysis, glycine, serine and threonine metabolism, purine metabolism, citrate cycle metabolism, *etc*. were possibly related to the etiology of colitis as well as the exacerbation by fenofibrate.

It was reported that an active inflammatory state leads to highly elevated energy expenditure due to enhanced protein catabolism[32, 33]. DSS-induced colitis mice suffered from diarrhea and muscle atrophy associated with enhanced protein catabolism, which may have caused the increases in amino acid levels[15]. At the same time, PPARα activation could also increase protein degradation, possibly results from its lipid-lowering action[19]. It was revealed that WY 14643, another PPARα agonist, raised total amino acid concentration (38%) in fat-fed rats, largely explained by glycine, serine and threonine increases[34]. In our study, in compatible with Ericsson's work[34], with the dual regulation of colitis and PPARα activation, up-regulation of

amino acids including serine, glycine and threonine was observed in colon of colitis mice, and was further potentiated after fenofibrate treatment.

Serine, glycine and threonine are three closely related amino acids that share common biochemical pathways. Threonine can be converted to glycine *via* THA. In this study, colon gene expression of THA was found to be significantly up-regulated in colitis mice and further potentiated in fenofibrate/DSS-treated WT mice, consistent with an increased colon glycine level in colitis mice and its further potentiation after fenofibrate treatment. This also indicated a possible correlation between PPARα activation and THA expression, which still awaits further study. Serine can be derived from four possible sources, and the pathway of serine utilization is a major source of one-carbon groups, in which glycine and 5,10-methylenetetrahydrofolate (5,10-MTHF) are generated [35]. In their work, Ericsson *et al*[34] attributed the WY 14643-induced increase of serine and glycine to boosted *de novo* synthesis of serine through phosphorylated intermediate pathway (where glycine was generated as a byproduct), cause genes including phosphoserine aminotransferase 1 (PSAT 1) were markedly up-regulated in liver and kidney of the rats[19,34]. In this study, colon PSAT1 expression was significantly increased in the fenofibrate-treated colitis group, consistent with the up-regulated serine and glycine levels for this group, and was in accordance with the previous literature[34]. Furthermore, serine is an important precursor for the synthesis of sphingolipids. Our previous lipidomic analysis revealed significantly increased bioactive sphingolipids in the colitis mice[9]. Therefore, the up-regulation of serine in colitis mice and its further potentiation after fenofibrate treatment may partly lead to the up-regulation of sphingolipids and are quite supportive to our previous lipidomics findings.

Deamination of amino acids in the liver releases ammonia, which is efficiently converted to nontoxic urea by the urea cycle[36]. In this study, increased urea levels were observed in both serum and colon of colitis mice, indicating an increased urea synthesis in IBD[37]. It was previously demonstrated that patients with active IBD often present with negative nitrogen balance because of high urinary nitrogen excretion[38], mostly urea-nitrogen[39], resulting in an up-regulated urea synthesis. After fenofibrate

treatment, the colitis mice had even higher urea level in serum/colon. This may due to PPARα mediated liver growth further increases the urea production capacity[19]. At the same time, colon uric acid level was increased in colitis mice. Uric acid is generated from the metabolism of purines[40], and its positive correlation with inflammation was found in a small clinical series of heart failure patients[41, 42], and a possible association between uric acid level and markers of inflammation in a population-based sample of participants was revealed, suggesting that uric acid might contribute to the proinflammatory state[43].

In this study, mice treated with DSS showed a decrease in body weight, and were subjected to rectal bleeding and diarrhea compared to controls. These observations suggest deficiencies of macronutrients, which is a common symptom observed in IBD[44]. Glucose serves as an energy source for normal intestinal mucosa[45]. In this study, a marked drop in serum glucose concentration mirrored the high energy deficit of the body and decreased energy availability due to decreased nutrient absorption through the impaired intestine[46], consistent with previous investigation[47]. At the same time, increased serum levels of citrate cycle intermediates (such as malic acid) indicated the high demand and rapid utilization of energy, and was synchronized with the boosted glycolysis to facilitate the increased rate of citrate cycle[46]

In addition, according to the correlation of serum and colon levels for the metabolite markers (Figure S2), some metabolites, such as glycine and isocitric acid, seemed to be positively correlated in serum and colon in the colitis mice; after fenofibrate-treatment, the correlation of serum and colon levels for some metabolites such as malic acid and urea were obviously increased, showing the further disturbed metabolism pathways as discussed above. The perturbed metabolic pathways revealed in this study was summarized in Figure 4.

Conclusion

In this study, GC-MS metabolomics was used to provide further insight into the PPARα-dependent exacerbation of colitis, with particular emphasis on changes in low-molecular-weight metabolites. With the aid of multivariate analysis and metabolic

pathway analysis, potential metabolite markers in amino acid metabolism, urea cycle, purine metabolism, and citrate cycle were highlighted. It was revealed that beyond control of lipid metabolism, PPARα also shows effects on the above pathways, resulting in enhanced protein catabolism, elevated energy expenditure, increased bioactive sphingolipid metabolism and proinflammatory state, which were possibly related to the exacerbated colitis.

Grants

This study was supported by National Science and Technology Major Project of the Ministry of Science and Technology of China (2013ZX09103-001-014), and Li-Shi-Zhen Young Scientist Project of School of Pharmacy at the Second Military Medical University, Shanghai, China.

Disclosures

The authors who have taken part in this study declared that they have nothing to disclose regarding funding or conflict of interest.

REFERENCES

1. **M. Aguilera, T. Darby and S. Melgar, The complex role of inflammasomes in the pathogenesis of Inflammatory Bowel Diseases – Lessons learned from experimental models, *Cytokine Growth F. R.* ,2014.**
2. **O. Abramson, M. Durant, W. Mow, A. Finley, P. Kodali, A. Wong, V. Tavares, E. McCroskey, L. Liu, J. D. Lewis, J. E. Allison, N. Flowers, S. Hutfless, F. S. Velayos, G. S. Perry, R. Cannon and L. J. Herrinton, Incidence, Prevalence, and Time Trends of Pediatric Inflammatory Bowel Disease in Northern California, 1996 to 2006, *J. Pediatr.* , 2010, 157, 233-239.e231.**
3. **A. Tursi, W. Elisei and M. Picchio, Incidence and prevalence of inflammatory bowel diseases in gastroenterology primary care setting, *Eur. J. Intern. Med.* , 2013, 24, 852-856.**
4. **A. D. Kraneveld, A. Rijnierse, F. P. Nijkamp and J. Garssen, Neuro-immune interactions in inflammatory bowel disease and irritable bowel syndrome: Future therapeutic targets, *Eur. J .Pharmacol.* , 2008, 585, 361-374.**
5. **M. Sobczak, A. Fabisiak, N. Murawska, E. Wesołowska, P. Wierzbicka, M. Wlazłowski, M. Wójcikowska, H. Zatorski, M. Zwolińska and J. Fichna, Current overview of extrinsic and intrinsic factors in etiology and progression of inflammatory bowel diseases, *Pharmacol .Rep.* , 2014, 66, 766-775.**

6. C. Duval, M. Müller and S. Kersten, PPARα and dyslipidemia, *BBA-Mol. Cell Biol. L.*, 2007, 1771, 961-971.
7. F. Zandbergen and J. Plutzky, PPARα in atherosclerosis and inflammation, *BBA-Mol. Cell. Biol. L.*, 2007, 1771, 972-982.
8. F. Rizvi, A. Puri, G. Bhatia, A. K. Khanna, E. M. Wulff, A. K. Rastogi and R. Chander, Antidyslipidemic action of fenofibrate in dyslipidemic–diabetic hamster model, *Biochem. Bioph.Res. Co.*, 2003, 305, 215-222.
9. Y. Qi, C. Jiang, N. Tanaka, K. W. Krausz, C. N. Brocker, Z.-Z. Fang, B. X. Bredell, Y. M. Shah and F. J. Gonzalez, PPARα-dependent exacerbation of experimental colitis by the hypolipidemic drug fenofibrate, *Am. J. Physiol-Gastr. L.*, 2014, 307, G564-G573.
10. K. Schoonjans, B. Staels and J. Auwerx, Role of the peroxisome proliferator-activated receptor (PPAR) in mediating the effects of fibrates and fatty acids on gene expression, *J .Lipid Res.*, 1996, 37, 907-925.
11. H. R. T. Williams, J. D. Willsmore, I. J. Cox, D. G. Walker, J. F. L. Cobbold, S. D. Taylor-Robinson and T. R. Orchard, Serum metabolic profiling in inflammatory bowel disease, *Digest. Dis. Sci.*, 2012, 57, 2157-2165.
12. F. Beigel, N. Teich, S. Howaldt, F. Lammert, J. Maul, S. Breiteneicher, C. Rust, B. Göke, S. Brand and T. Ochsenkühn, Colesevelam for the treatment of bile acid malabsorption-associated diarrhea in patients with Crohn's disease: A randomized, double-blind, placebo-controlled study, *J .Crohn's Colitis*, 2014, 8, 1471-1479.
13. F. Fernández-Bañares, M. Esteve-Comas, J. Mañé, E. Navarro, X. Bertrán, E. Cabré, R. Bartolí, J. Boix, C. Pastor and M. A. Gassull, Changes in mucosal fatty acid profile in inflammatory bowel disease and in experimental colitis: a common response to bowel inflammation, *Clin. Nutr.*, 1997, 16, 177-183.
14. M. Ooi, S. Nishiumi, T. Yoshie, Y. Shiomi, M. Kohashi, K. Fukunaga, S. Nakamura, T. Matsumoto, N. Hatano, M. Shinohara, Y. Irino, T. Takenawa, T. Azuma and M. Yoshida, GC/MS-based profiling of amino acids and TCA cycle-related molecules in ulcerative colitis, *Inflamm. Res.*, 2011, 60, 831-840.
15. Y. Shiomi, S. Nishiumi, M. Ooi, N. Hatano, M. Shinohara, T. Yoshie, Y. Kondo, K. Furumatsu, H. Shiomi, H. Kutsumi, T. Azuma and M. Yoshida, GCMS-based metabolomic study in mice with colitis induced by dextran sulfate sodium, *Inflamm. Bowel Dis.*, 2011, 17, 2261-2274.
16. R. Schicho, R. Shaykhutdinov, J. Ngo, A. Nazyrova, C. Schneider, R. Panaccione, G. G. Kaplan, H. J. Vogel and M. Storr, Quantitative metabolomic profiling of serum, plasma, and urine by (1)H NMR spectroscopy discriminates between patients with inflammatory bowel disease and healthy individuals, *J. Proteome Res.*, 2012, 11, 3344-3357.
17. F. Gothe, F. Beigel, C. Rust, M. Hajji, S. Koletzko and F. Freudenberg, Bile acid malabsorption assessed by 7 alpha-hydroxy-4-cholesten-3-one in pediatric inflammatory bowel disease: Correlation to clinical and laboratory findings, *J.Crohn's Colitis*, 2014, 8, 1072-1078.
18. S. Heimerl, C. Moehle, A. Zahn, A. Boettcher, W. Stremmel, T. Langmann and G. Schmitz, Alterations in intestinal fatty acid metabolism in inflammatory bowel disease, *BBA-Mol. Cell Biol. L.*, 2006, 1762, 341-350.
19. K. Sheikh, G. Camejo, B. Lanne, T. Halvarsson, M. R. Landergren and N. D. Oakes, Beyond lipids, pharmacological PPARalpha activation has important effects on amino acid metabolism as studied in the rat, *Am J physiol: Endocrin. Met.*, 2007, 292, E1157-1165.

20. G. D. Lewis, A. Asnani and R. E. Gerszten, Application of Metabolomics to Cardiovascular Biomarker and Pathway Discovery, *J. Am. Coll. Cardiol.*, 2008, 52, 117-123.
21. M. P. Quinones and R. Kaddurah-Daouk, Metabolomics tools for identifying biomarkers for neuropsychiatric diseases, *Neurobiol. Dis.*, 2009, 35, 165-176.
22. S. Moco, J. Vervoort, S. Moco, R. J. Bino, R. C. H. De Vos and R. Bino, Metabolomics technologies and metabolite identification, *TrAC-Trend Anal. Chem.*, 2007, 26, 855-866.
23. K. K. Pasikanti, P. C. Ho and E. C. Y. Chan, Gas chromatography/mass spectrometry in metabolic profiling of biological fluids, *J. Chromatogr., B*, 2008, 871, 202-211.
24. K. Bando, R. Kawahara, T. Kunimatsu, J. Sakai, J. Kimura, H. Funabashi, T. Seki, T. Bamba and E. Fukusaki, Influences of biofluid sample collection and handling procedures on GC–MS based metabolomic studies, *J. Biosci. Bioeng.*, 2010, 110, 491-499.
25. H. Tsugawa, T. Bamba, M. Shinohara, S. Nishiumi, M. Yoshida and E. Fukusaki, Practical non-targeted gas chromatography/mass spectrometry-based metabolomics platform for metabolic phenotype analysis, *J. Biosci. Bioeng.*, 2011, 112, 292-298.
26. H. Tsugawa, Y. Tsujimoto, K. Sugitate, N. Sakui, S. Nishiumi, T. Bamba and E. Fukusaki, Highly sensitive and selective analysis of widely targeted metabolomics using gas chromatography/triple-quadrupole mass spectrometry, *J. Biosci. Bioeng.*, 2014, 117, 122-128.
27. H. S. Cooper, S. N. Murthy, R. S. Shah and D. J. Sedergran, Clinicopathologic study of dextran sulfate sodium experimental murine colitis, *Lab. Invest.* , 1993, 69, 238-249.
28. I. Okayasu, S. Hatakeyama, M. Yamada, T. Ohkusa, Y. Inagaki and R. Nakaya, A novel method in the induction of reliable experimental acute and chronic ulcerative colitis in mice, *Gastroenterology*, 1990, 98, 694-702.
29. Y. Qi, H. Gu, Y. Song, X. Dong, A. Liu, Z. Lou, G. Fan and Y. Chai, Metabolomics Study of Resina Draconis on Myocardial Ischemia Rats Using Ultraperformance Liquid Chromatography/Quadrupole Time-of-Flight Mass Spectrometry Combined with Pattern Recognition Methods and Metabolic Pathway Analysis, *Evid-based Compl. Alt.: eCAM*, 2013, 2013, 438680.
30. N. Monschau, K. P. Stahmann, H. Sahm, J. B. McNeil and A. L. Bognar, Identification of Saccharomyces cerevisiae GLY1 as a threonine aldolase: a key enzyme in glycine biosynthesis, *FEMS Microbiol.*, 1997, 150, 55-60.
31. A. J. A. van Maris, M. A. H. Luttik, A. A. Winkler, J. P. van Dijken and J. T. Pronk, Overproduction of threonine aldolase circumvents the biosynthetic role of pyruvate decarboxylase in glucose-limited chemostat cultures of Saccharomyces cerevisiae, *Appl. Environ. Microb.*, 2003, 69, 2094-2099.
32. T. A. Lennie, Relationship of body energy status to inflammation-induced anorexia and weight loss, *Physiol. Behav.*, 1998, 64, 475-481.
33. N. Le Floc'h, D. Melchior and C. Obled, Modifications of protein and amino acid metabolism during inflammation and immune system activation, *Livest. Prod. Sci.*, 2004, 87, 37-45.
34. A. Ericsson, N. Turner, G. I. Hansson, K. Wallenius and N. D. Oakes, Pharmacological PPARα Activation Markedly Alters Plasma Turnover of the Amino Acids Glycine, Serine and Arginine in the Rat, *PLoS ONE*, 2014, 9, e113328.
35. T. J. de Koning, S. A. Fuchs and L. W. J. Klomp, in *Handbook of Neurochemistry and Molecular Neurobiology*, eds. A. Lajtha, S. Oja, A. Schousboe and P. Saransaari, Springer US,

2007.

36. S. Kersten, S. Mandard, P. Escher, F. J. Gonzalez, S. Tafuri, B. Desvergne and W. Wahli, The peroxisome proliferator-activated receptor alpha regulates amino acid metabolism, *FASEB J.*, 2001, 15, 1971-1978.

37. K. Thomsen, H. Grønbæk, J. Dahlerup, N. Aagaard, L. Christensen, J. Agnholt, J. Frystyk and H. Vilstrup, Prednisolone but not infliximab aggravates the upregulated hepatic nitrogen elimination in patients with active inflammatory bowel disease, *Inflamm. Bowel Dis.*, 2014, 20, 7-13.

38. S. Klein, S. Meyers, P. O'Sullivan, D. Barton, N. Leleiko and H. Janowitz, The metabolic impact of active ulcerative colitis. Energy expenditure and nitrogen balance, *J. Clin. Gastroenterol.*, 1988, 10, 34-40.

39. C. Lundsgaard, O. Hamberg, O. Ø. Thomsen, O. H. Nielsen and H. Vilstrup, Increased hepatic urea synthesis in patients with active inflammatory bowel disease, *J. Hepatol.*, 1996, 24, 587-593.

40. A. Mandal and D. B. Mount, The Molecular Physiology of Uric Acid Homeostasis, *Annu. Rev. Physiol.*, 2013.

41. F. Leyva, S. D. Anker, I. F. Godsland, M. Teixeira, P. G. Hellewell, W. J. Kox, P. A. Poole-Wilson and A. J. Coats, Uric acid in chronic heart failure: a marker of chronic inflammation, *Eur. Heart J.*, 1998, 19, 1814-1822.

42. P. Olexa, M. Olexova, J. Gonsorcik, I. Tkac, J. Kisel'ova and M. Olejnikova, Uric acid-a marker for systemic inflammatory response in patients with congestive heart failure?, *Wien. Klin. Wochenschr.*, 2002, 114, 211-215.

43. C. Ruggiero, A. Cherubini, A. Ble, A. J. G. Bos, M. Maggio, V. D. Dixit, F. Lauretani, S. Bandinelli, U. Senin and L. Ferrucci, Uric acid and inflammatory markers, *Eur. Heart J.*, 2006, 27, 1174-1181.

44. S. Massironi, R. E. Rossi, F. A. Cavalcoli, S. Della Valle, M. Fraquelli and D. Conte, Nutritional deficiencies in inflammatory bowel disease: Therapeutic approaches, *Clin. Nutr.*, 2013, 32, 904-910.

45. W. Roediger, Utilization of nutrients by isolated epithelial cells of the rat colon, *Gastroenterology*, 1982, 83, 424-429.

46. F. Dong, L. Zhang, F. Hao, H. Tang and Y. Wang, Systemic Responses of Mice to Dextran Sulfate Sodium-Induced Acute Ulcerative Colitis Using 1H NMR Spectroscopy, *J. Proteome Res.*, 2013, 12, 2958-2966.

47. R. Schicho, A. Nazyrova, R. Shaykhutdinov, G. Duggan, H. J. Vogel and M. Storr, Quantitative Metabolomic Profiling of Serum and Urine in DSS-Induced Ulcerative Colitis of Mice by 1H NMR Spectroscopy, *J. Proteome Res.*, 2010, 9, 6265-6273.

Table.1 Identified metabolite markers in the serum (colon) of colitis mice.

NO	Retention time (min)	m/z	ID	Identification results	B *vs.* A	C *vs.* B	D *vs.* C	Pathway
1	17.42	147.1116	C00149	Malic acid	↑*	↑	↓	Citrate cycle
2	10.8	188.9971	C00086	Urea	↑** (↑)	↑(↑)	↓(↓)	Purine metabolism
3	8.42	146.9984	C00209	Oxalic acid	↓	↓	↑	Glyoxylate and dicarboxylate metabolism
4	30.05	147.1917	C00031	Glucose	↓*	↓**	↑	Glycolysis / Gluconeogenesis
5	27.27	273.1575	C00311	Isocitric acid	↑	↓	↑	Citrate cycle
6	35.81	305.1802	C00137	Myoinositol	↑(↓*)	↓(↓)	↑(↑)	Inositol phosphate metabolism
7	7.87	147.1257	C00037	Glycine	(↑*)	(↑)	(↓)	Glycine, serine and threonine metabolism
8	14.12	204.1879	C00065	Serine	(↑)	(↑)	(↓)	Glycine, serine and threonine metabolism
9	14.82	218.1231	C00188	Threonine	(↑)	(↑)	(↓)	Glycine, serine and threonine metabolism
10	8.88	147.1195	C00246	Butanoic acid	(↑**)	(↑*)	(↓)	Butanoate metabolism
11	35.92	147.1106	C00366	Uric acid	(↑)	(↑**)	(↓)	Purine metabolism
12	26.1	265.2826	C15587	Purine	(↓**)	(↓)	(↑)	Purine metabolism

A, B, C, and D represent control mice, DSS-treated WT mice, fenofibrate/DSS-treated WT and fenofibrate/DSS-treated Ppara-null mice, respectively;

↑ or ↓ represents the up- or down-regulation of the metabolites in serum; ↑ or ↓ in brackets represent the up- or down-regulation of the metabolite leves in colon. (*p< 0.05, **p< 0.01).

FIGURE LEGENDS

Figure 1. A. PCA scores plot (with the cumulative R^2X 0.659 and Q^2 0.543) and B. PLS-DA scores plot (with the cumulative R^2X 0.771, R^2Y 0.841, and Q^2 0.442) of serum samples from all the four examined groups, *i.e.* control (WT-CTR/Water), colitis (WT-CTR/DSS), fenofibrate-treated colitis (WT-FF/DSS on WT mice and KO-FF/DSS on PPARα-null (KO) mice). C. PCA scores plot (with the cumulative R^2X 0.602 and Q^2 0.196) and D. PLS-DA scores plot (with the cumulative R^2X 0.818, R^2Y 0.99, and Q^2 0.763) of colon samples for the four examined groups.

Figure 2. Target quantitation of significantly changed metabolites in serum and colon based on standard curves using authentic standards. A. serum metabolites levels in the examined groups. B. colon metabolites levels in the examined groups. Data were expressed as mean ± SD. *p< 0.05 and **p< 0.01.

Figure 3. Quantitative real time PCR analysis of colon THA and PSAT1 mRNA expression in control (WT-CTR/Water), colitis (WT-CTR/DSS), fenofibrate-treated colitis (WT-FF/DSS on WT mice and KO-FF/DSS on PPARα-null (KO) mice). Data were expressed as mean±SD. *Indicates p<0.05 and **indicates p<0.01. Abbreviations: THA, threonine aldolase; PSAT1, phosphoserine aminotransferase 1.

Figure 4. Schematic representation of the metabolic pathways. Metabolites in bold black were revealed as potential metabolite markers in this study, and the column values in histograms were expressed as mean±SD of their relative levels. Sphingomyelins (SM) and ceramides in sphingolipid metabolism were reported in our previous study. Metabolites in italic were not detected in this study.

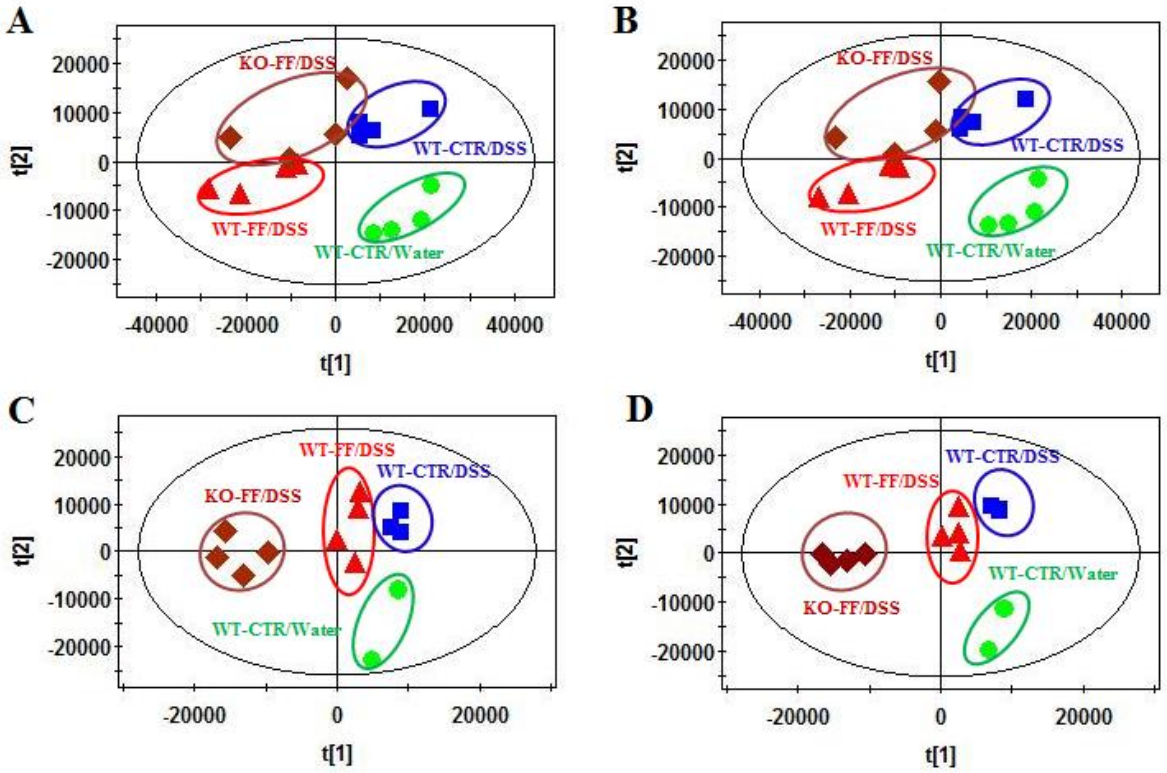

Figure 1. A. PCA scores plot (with the cumulative R^2X 0.659 and Q^2 0.543) and B. PLS-DA scores plot (with the cumulative R^2X 0.771, R^2Y 0.841, and Q^2 0.442) of serum samples from all the four examined groups, *i.e.* control (WT-CTR/Water), colitis (WT-CTR/DSS), fenofibrate-treated colitis (WT-FF/DSS on WT mice and KO-FF/DSS on PPARα-null (KO) mice). C. PCA scores plot (with the cumulative R^2X 0.602 and Q^2 0.196) and D. PLS-DA scores plot (with the cumulative R^2X 0.818, R^2Y 0.99, and Q^2 0.763) of colon samples for the four examined groups..

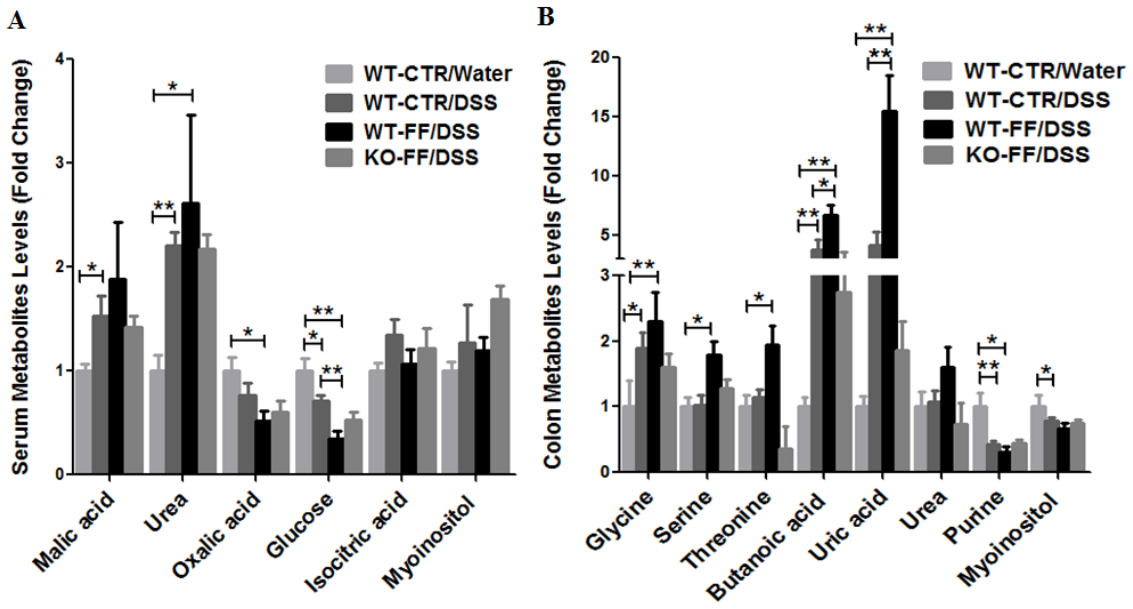

Figure 2. Target quantitation of significantly changed metabolites in serum and colon based on standard curves using authentic standards. A. serum metabolites levels in the examined groups. B. colon metabolites levels in the examined groups. Data were expressed as mean ± SD. *p< 0.05 and **p< 0.01.

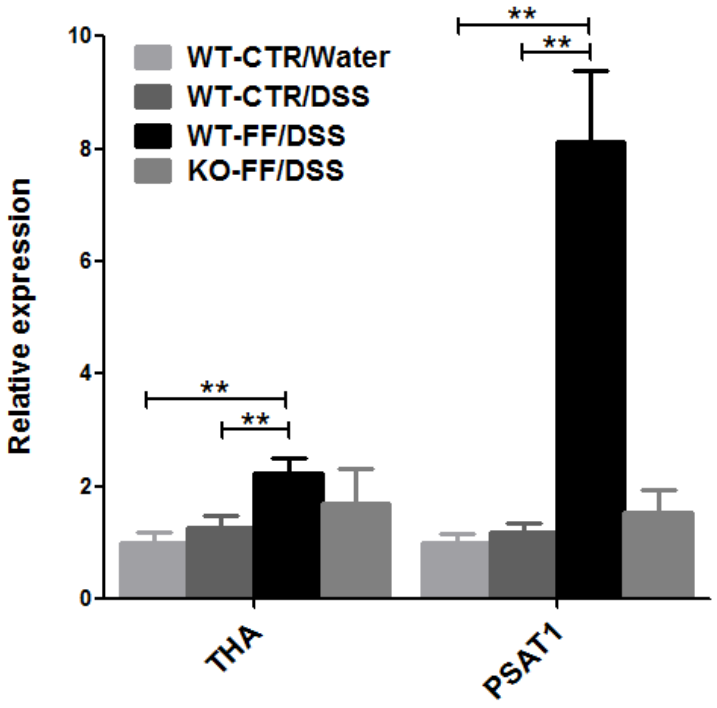

Figure 3. Quantitative real time PCR analysis of colon THA and PSAT1 mRNA expression in control (WT-CTR/Water), colitis (WT-CTR/DSS), fenofibrate-treated colitis (WT-FF/DSS on WT mice and KO-FF/DSS on PPARα-null (KO) mice). Data were expressed as mean±SD. *Indicates $p<0.05$ and **indicates $p<0.01$. Abbreviations: THA, threonine aldolase; PSAT1, phosphoserine aminotransferase 1.

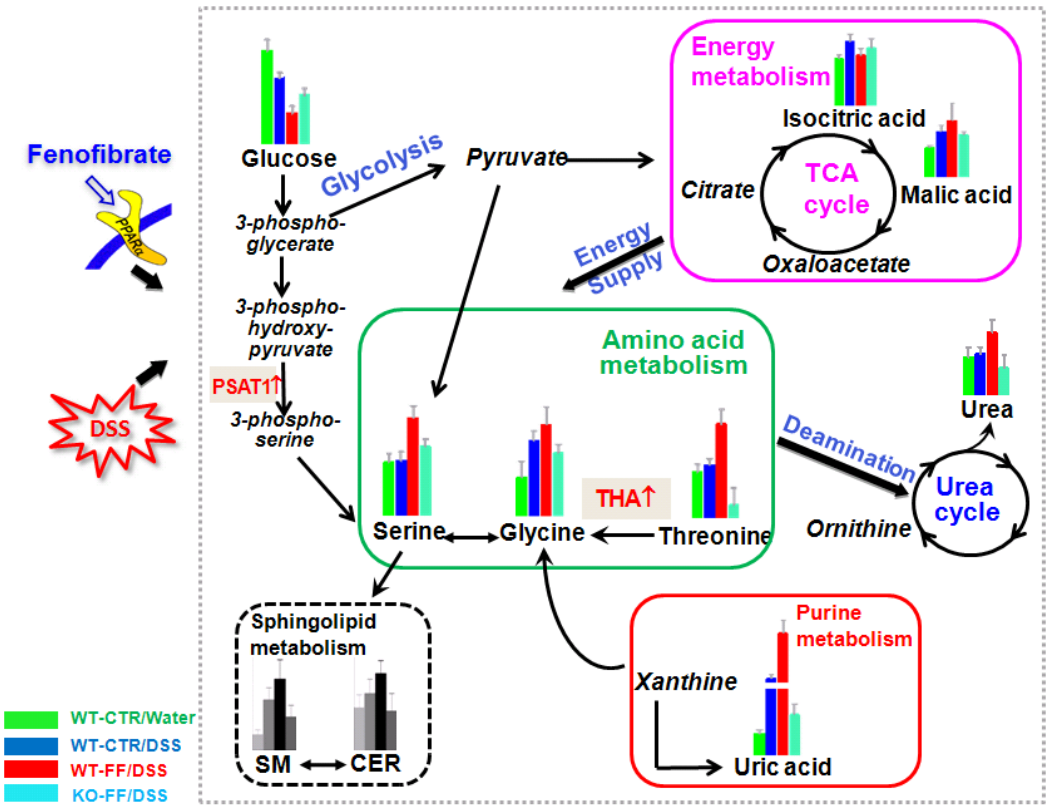

Figure 4. Schematic representation of the metabolic pathways. Metabolites in bold black were revealed as potential metabolite markers in this study, and the column values in histograms were expressed as mean±SD of their relative levels. Sphingomyelins (SM) and ceramides in sphingolipid metabolism were reported in our previous study. Metabolites in italic were not detected in this study.